*Acta Cryst.* (1969). A25, 319

# Analytical Evaluation of Thermal Diffuse Scattering Contributions to Integrated X-ray Intensities in the Vicinity of a Bragg Reflection*†

BY EARL F. SKELTON

*U. S. Naval Research Laboratory, Washington, D. C.* 20390, *U.S.A.*

AND J. LAWRENCE KATZ

*The Laboratory for Crystallographic Research, Department of Physics and Astronomy, Rensselaer Polytechnic Institute, Troy, New York* 12181, *U.S.A.*

(*Received* 3 *April* 1968)

The first order thermal diffuse scattering contribution to integrated Bragg scattering intensities for monatomic, crystalline lattices has been analytically evaluated. Parallel arguments for evaluation of the integrated Bragg intensity and the integrated thermal diffuse scattering intensity are developed for a general diffractometer intensity scan. The resulting general expressions are reduced to a simplified form for several situations. In particular, the two standard integrated intensity scans, an $\omega$-scan and an $\omega/2\theta$-scan, are considered. Comparison is made between the results of this calculation and previously published calculations, as well as with recently published experimental measurements of thermal diffuse scattering effects. The variation of the thermal diffuse scattering contributions to the measured intensity is discussed through consideration of a dimensionless parameter, which is independent of both temperature and the diffracting material. This parameter depends only on the experimental constants relating to the intensity measurement and is examined as a function of the detection window size, the scan width and type, and the diffraction angle. It is found, for the situations considered, that the ratio of the thermal diffuse scattering to the Bragg scattering tends to show a pronounced maximum in the intermediate-high angle region ($60° \lesssim \theta \lesssim 80°$).

## Introduction

Scattered X-radiation from a crystalline lattice can be analytically decomposed into two major types: Bragg scattering, and thermal diffuse scattering (T.D.S.). The Bragg scattering owes its origin to the periodicity of the crystalline lattice while the T.D.S. arises from an interaction between the incident X-radiation and the thermal lattice waves of the crystal. As the temperature of the crystal approaches absolute zero, the Bragg scattering approaches a maximum, whereas the T.D.S. tends to vanish. Furthermore, as the scattering vector approaches a reciprocal lattice point corresponding to an allowed reflection, both the Bragg scattering and the T.D.S. will approach maxima, although the former will be much sharper. Because these two effects are maximized simultaneously, it is difficult to separate the Bragg scattering and the T.D.S. experimentally; this separation is therefore usually performed analytically.

The basic theory involved in calculating T.D.S. effects was originally developed by Waller (1925, 1928). Warren (1953) and Chipman & Paskin (1959) have developed techniques for correction of the T.D.S. for crystalline powders. Nicklow & Young (1964) have carried out a rather extensive calculation of the T.D.S. contribution for peak intensity measurements, utilizing a weighting function to describe the net T.D.S. contribution from each point in reciprocal space.

Nilsson (1957) carried out one of the first calculations of the T.D.S. effect for integrated, single-crystal, diffractometer intensity measurements. Expanding on Waller's original work, Nilsson developed a method of evaluating the integrated first order T.D.S. from simple cubic single-crystals, neglecting possible anisotropy and assuming an X-ray detection window of infinite height. Schwartz (1964) has pointed out that Nilsson's expressions tacitly assume a specific relation between the elastic constants, which is not valid for many metals; he has proposed a modified expression for such situations. Annaka (1962) has extended Nilsson's treatment to include not only consideration of electronically measured intensities from rotating crystals ($\omega$-scan), but photographic intensity measurements as well. However, in order to simplify subsequent calculations, Annaka, as Nilsson, assumes a simpler shape for the detection window than actually exists. Cooper & Rouse (1968) have recently improved upon Nilsson's calculation by considering an $\omega/2\theta$-scan; they have also evaluated the errors involved in assuming an infinitely high detector window.

These earlier calculations are somewhat restrictive in that they are limited to materials crystallizing in the cubic system and consider only specific types of inte-

---

* A portion of this work was carried out while E.F.S. was pursuing an National Academy of Sciences–National Research Council Postdoctoral Research Associateship.

† This work was supported in part by the National Aeronautics and Space Administration through the Rensselaer Interdisciplinary Materials Research Center, the National Institute of Dental Research under Grants 5T1 DE 117-04 and 5P01 02336-02, and the Army Research Office (Durham).

grated intensity scans. In this work, a correction for the T.D.S. will be developed which (1) is presumed to be applicable to all crystalline classes, (2) will consider a general, diffractometer integrated intensity scan in the vicinity of a reciprocal lattice point, and (3) will employ a somewhat simpler and more general expression for evaluation of the mean reciprocal square of the lattice wave velocity from elastic constant data. Based on existing theory, the calculation of both the Bragg scattering intensity and the T.D.S. intensity will be developed together.

## Theory

The object of the following analysis is to represent the intensity scattered from a small single-crystallite which is completely bathed in an incident beam of X-radiation. It is assumed that: the kinematical theory of X-ray scattering is applicable; the adiabatic (or Born–Oppenheimer) approximation is valid; the quasi-harmonic approximation can be employed. Further, in relating the results of this calculation to that which is actually measured in the laboratory (the integrated intensity) it is assumed that the intensity contributions from each of the constituent mosaic blocks in the real crystal (which is believed to be composed of many crystallites) will sum in the same manner for the Bragg scattering and the T.D.S. This last assumption merely presumes that the ratio of the integrated T.D.S. to the integrated Bragg scattering will be the same for each mosaic block in the real crystal.

There are a number of excellent developments of the general theory of the scattering of X-rays from a crystalline lattice, *cf.* Born (1943), James (1962), Maradudin, Montroll & Weiss (1963), and Nicklow & Young (1964). The notation of James (1962) will be employed in this discussion. Restricting this development to Bravais lattices, the intensity scattered from a crystalline lattice can be expressed as follows:

$$<I(\mathbf{S}/\lambda)> = C|f_0|^2 e^{-2M}[I_0(\mathbf{S}/\lambda) + \sum_{n=1}^{\infty} I_{\mathrm{TDS}-n}] \quad (1)$$

where $C$ includes a number of constant terms including the Thomson expression for a radiating electron, the polarization factor, and the intensity of the incident X-ray beam; $f_0$ is the atomic scattering factor; $\mathbf{S}$ is the diffraction vector; $\lambda$ is the wavelength of the X-radiation. The exponential term in equation (1) is commonly referred to as the Debye–Waller factor and represents the primary thermal influence on the scattered radiation. $I_0(\mathbf{S}/\lambda)$ is the Laue interference function and represents the Bragg scattering; the $n$th term in the series, $I_{\mathrm{TDS}-n}$, is the $n$th order T.D.S. contribution to the scattered intensity. More specifically, $I_{\mathrm{TDS}-n}$ represents an interaction between an X-ray photon and $n$ lattice wave phonons. Clearly the probability of the occurrence of multi-phonon collisions is significantly less than that associated with the first or second order T.D.S.; in the following calculation, only the first order contribution will be considered.

The first order T.D.S. can be expressed in terms of the crystalline lattice waves in a Bravais lattice as follows:

$$I_{\mathrm{TDS}-1} = \frac{1}{2mN} \sum_{\mathbf{k}} \sum_{j=1}^{3} \left[ \left\{ \frac{\mathbf{S}}{\lambda} \cdot \hat{\mathbf{e}}\left(\begin{matrix}\mathbf{k}\\ j\end{matrix}\right) \right\}^2 \times <E\left(\begin{matrix}\mathbf{k}\\ j\end{matrix}\right)> \Big/ v\left(\begin{matrix}\mathbf{k}\\ j\end{matrix}\right)^2 \cdot \{I_0(\mathbf{S}/\lambda+\mathbf{g}) + I_0(\mathbf{S}/\lambda-\mathbf{g})\} \right] \quad (2)$$

where

$$\mathbf{k} = 2\pi\mathbf{g} \quad (3)$$

$N$ is the number of atoms in the lattice; $m$ is the atomic mass; $\hat{\mathbf{e}}\left(\begin{matrix}\mathbf{k}\\ j\end{matrix}\right)$ is the unit polarization vector associated with the normal mode of polarization index $j$ and of wave vector $\mathbf{k}$; $<E\left(\begin{matrix}\mathbf{k}\\ j\end{matrix}\right)>$ is the mean energy associated with that particular wave component and is given by the following expression:

$$<E\left(\begin{matrix}\mathbf{k}\\ j\end{matrix}\right)> = \frac{1}{2} h v\left(\begin{matrix}\mathbf{k}\\ j\end{matrix}\right) \coth\left[ h v\left(\begin{matrix}\mathbf{k}\\ j\end{matrix}\right) \Big/ 2kT \right] \quad (4)$$

where $v\left(\begin{matrix}\mathbf{k}\\ j\end{matrix}\right)$ is the frequency associated with the same wave component; $T$ is the absolute temperature; $h$ and $k$ are Planck's and Boltzmann's constants respectively. The function $I_0(\mathbf{S}/\lambda \pm \mathbf{g})$ in equation (2) is similar to the standard Laue interference function. However, instead of peaking at a reciprocal lattice point, it has a very sharp maximum at the vector distance $\pm\mathbf{g}$ from the reciprocal lattice point. Following the example of Maradudin *et al.* (1963), the Laue interference function is replaced by a delta function:

$$I_0(\mathbf{X}) = N^2 \Delta(\mathbf{X}) \quad (5)$$

where $\Delta(\mathbf{X})$ is zero unless $\mathbf{X}$ terminates on a reciprocal lattice point, in which case it is unity. Thus, equation (2) takes the form:

$$I_{\mathrm{TDS}-1} = \frac{N}{2m} \sum_{\mathbf{k}} \sum_{j=1}^{3} \left[ \left\{ \frac{\mathbf{S}}{\lambda} \cdot \hat{\mathbf{e}}\left(\begin{matrix}\mathbf{k}\\ j\end{matrix}\right) \right\}^2 \times <E\left(\begin{matrix}\mathbf{k}\\ j\end{matrix}\right)> \Big/ v\left(\begin{matrix}\mathbf{k}\\ j\end{matrix}\right)^2 \cdot \{\Delta(\mathbf{S}/\lambda+\mathbf{g}) + \Delta(\mathbf{S}/\lambda-\mathbf{g})\} \right]. \quad (6)$$

Consider the first order T.D.S. at a point in reciprocal space defined by the vector $\mathbf{S}/\lambda$, this point being in the vicinity of some reciprocal lattice point. Realizing that the information regarding the wave vectors of the normal vibration modes is completely contained within a Brillouin zone, the summation over $\mathbf{k}$ need only be performed over the Brillouin zone surrounding the reciprocal lattice point in question. When this summation is carried out, there will be one, and only one, wave vector which will yield a non-vanishing contribution from the first term in equation (6). Call this $\mathbf{g}'$, that is, $\mathbf{S}/\lambda + \mathbf{g}'$ will terminate on the reciprocal lattice

point in question. Similarly, the only non-vanishing contribution from the second term will come from $-\mathbf{g}'$. Therefore, summation over all lattice waves, for a particular diffraction vector, gives:

$$I_{\mathrm{TDS}-1}(\mathbf{S}/\lambda)=\frac{N}{m}\sum_{j=1}^{3}\left[\left\{\frac{\mathbf{S}}{\lambda}\cdot\hat{\mathbf{e}}\left(\frac{\mathbf{k}}{j}\right)\right\}^2 \times <E\left(\frac{\mathbf{k}}{j}\right)>\Big/\nu\left(\frac{\mathbf{k}}{j}\right)^2\right] \quad (7)$$

Resubstitution into equation (1) then yields the following expression for the energy scattered per unit area per unit time at a point defined by the vector $\bar{\mathbf{S}}/\lambda$ (to first order in the T.D.S.):

$$<I(\mathbf{S}/\lambda)> = C|f_0|^2e^{-2M}\left[I_0(\mathbf{S}/\lambda) + \frac{N}{m}\sum_{j=1}^{3}\left[\left\{\frac{\mathbf{S}}{\lambda}\cdot\hat{\mathbf{e}}\left(\frac{\mathbf{k}}{j}\right)\right\}^2 <E\left(\frac{\mathbf{k}}{j}\right)>\Big/\nu\left(\frac{\mathbf{k}}{j}\right)^2\right]\right] \quad (8)$$

where it is required that the wave vector, $\bar{\mathbf{k}}$, has the property that $\mathbf{S}/\lambda+\mathbf{g}$ terminates on a reciprocal lattice point [$\mathbf{k}$ is related to $\mathbf{g}$ in equation (3)].

*Integrated intensity*

The quantity which is usually measured is the total energy, or integrated intensity; that is, in measuring Bragg reflections, it is standard procedure to move the diffracting crystal and/or the X-ray detection aperture through some small region surrounding the Bragg peak under investigation. This experimental integration of the intensity corresponds to integrating the function $<I(\mathbf{S}/\lambda)>$ over the equivalent region in reciprocal space.

The integration of the first term in equation (8) is fairly straightforward. Since the Laue interference function is very sharply peaked at the reciprocal lattice point, the result is independent of the shape and size of the region over which the integration is carried out, so long as it is large enough adequately to cover the Bragg peak itself.

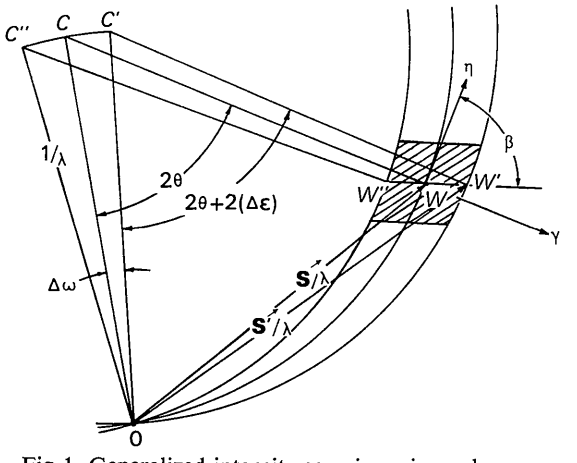


Fig. 1. Generalized intensity scan in reciprocal space.

In carrying out the integration of equation (8), a completely general diffractometer intensity scan will be considered, *i.e.* it is assumed that the intensity is measured as the crystal rotates about the $\omega$ axis through the angle $\omega$ and as the detector aperature simultaneously rotates about the same axis through the angle $\varepsilon$. This situation in reciprocal space is depicted schematically in Fig. 1. The origin of the reciprocal lattice is located at point $O$; the circular lines running through point $O$ represent portions of the intersection of the Ewald sphere of reflection of radius $1/\lambda$, and the diffraction plane. As the intensity is scanned in the manner described above, the diffraction vector, $\mathbf{S}/\lambda$, moves from the point $W$ to the point $W'$. This general intensity scan can be reduced to either of the two standard intensity integration procedures: An $\omega$ scan, in which only the crystal rotates, corresponds to $\varepsilon=0$ and an $\omega/2\theta$ scan, in which the crystal and detector rotate in a 1:2 ratio, arises when $\varepsilon=\omega$.

An orthogonal, right-handed coordinate system is established at $W$ by the quantities $(H,X,\Gamma)$; the corresponding directions are defined by the three unit vectors: $\hat{\mathbf{e}}_H$, $\hat{\mathbf{e}}_X$, and $\hat{\mathbf{e}}_\Gamma$. The positive $\hat{\mathbf{e}}_\Gamma$ direction lies in the diffraction plane, is orthogonal to the Ewald sphere at the point $W$, and is directed outward from the Ewald sphere. The other two directions are tangential to the Ewald sphere at $W$; $\hat{\mathbf{e}}_H$ lies in the diffraction plane directed away from the origin and $\hat{\mathbf{e}}_X$ is formed from the cross-product: $\hat{\mathbf{e}}_\Gamma\times\hat{\mathbf{e}}_H$. The two directions $\hat{\mathbf{e}}_H$ and $\hat{\mathbf{e}}_X$ correspond to the detector window width and height, respectively. If the point $W$ represents the reciprocal lattice point associated with the Bragg peak under investigation, then as the integrated intensity is measured, a volume element, centered at $W$, will be swept out; the projection of this volume onto the diffraction plane is shown cross-hatched in Fig. 1. Considering half of the intensity scan first, *i.e.* the situation as the diffraction vector changes from $\mathbf{S}/\lambda$ to $\mathbf{S}'/\lambda$, the limits on the intensity scan can be written as follows:

$$\left.\begin{aligned} H_1&=-\frac{1}{\lambda}\tan(\Delta\eta/2)+\Gamma\cot\beta;\\ H_2&=+\frac{1}{\lambda}\tan(\Delta\eta/2)+\Gamma\cot\beta\\ X_1&=-\frac{1}{\lambda}\tan(\Delta\chi/2);\ X_2=+\frac{1}{\lambda}\tan(\Delta\chi/2)\\ \Gamma_1&=0;\ \Gamma_2=\frac{1}{\lambda}\Delta\xi\sin\beta \end{aligned}\right\} \quad (9)$$

where $\Delta\eta$ and $\Delta\chi$ are the angular width and height, respectively, of the detection window. $\xi/\lambda$ refers to the quantity $\left|\frac{\mathbf{S}'}{\lambda}-\frac{\mathbf{S}}{\lambda}\right|$; from the geometry of Fig. 1, $\xi$ can be expressed in terms of $\omega$ and $\varepsilon$ by the following:

$$\xi=2[\sin^2(\theta+\varepsilon)+\sin^2\theta-2\sin(\theta+\varepsilon) \times\sin\theta\cos(\omega-\varepsilon)]^{1/2}. \quad (10)$$

Also, the angle between $\xi$ and $\hat{\mathbf{e}}_H$ ($\beta$) can be written as

follows:

$$\beta = \frac{\pi}{2} + \theta - \arccos\left\{\frac{4}{\xi}\sin\theta\sin\left(\frac{\omega-\varepsilon}{2}\right)\right\} \quad (11)$$

If the angular displacements, $\omega$ and $\varepsilon$, are reasonably small in comparison with unity, then these expressions can be reduced to a somewhat simpler form, *viz*:

$$\xi \simeq 2[\varepsilon^2 + (\omega^2 - 2\omega\varepsilon)\sin^2\theta]^{1/2} \quad (10')$$

$$\beta \simeq \frac{\pi}{2} + \theta - \arccos\left\{\frac{2}{\xi}(\omega-\varepsilon)\sin\theta\right\} \quad (11')$$

Further, if the detector windows angular dimensions are sufficiently small, then the tangent functions in equation (9) can be replaced by the angles themselves.

Let us first consider the integrated Bragg intensity. For a particular position of the X-ray detection window, *i.e.* a particular value of the diffraction vector, the Bragg scattering energy measured per unit time is given by the following:

$$\frac{dJ_{\text{Bragg}}}{dt} = C|f_0|^2 e^{-2M}\int_\eta\int_\chi R^2 I_0(\mathbf{S}/\lambda)\,d\eta\,d\chi \quad (12)$$

where $R$ is the distance between the crystal and the detection window, *i.e.* the radius of the diffractometer (it is presumed that the detection window is normal to the scattered beam and that $R$ is large compared to the size of the crystallite). The total measured Bragg energy is then determined by integrating equation (12) over the time interval involved:

$$J_{\text{Bragg}} = CR^2|f_0|^2 e^{-2M}\int_\eta\int_\chi\int_t I_0(\mathbf{S}/\lambda)\,d\eta\,d\chi\,dt$$

$$= CR^2|f_0|^2 e^{-2M}\int_\eta\int_\chi\int_\xi I_0(\mathbf{S}/\lambda)\,d\eta\,d\chi\,\frac{d\xi}{\dot\xi} \quad (13)$$

where the time rate of change of $\xi$, $\dot\xi$, is assumed to be constant, *i.e.* the rotations described by $\omega$ and/or $\varepsilon$ are presumed to be constant in time.

The variables of the integration can be expressed in the previously defined coordinate system as follows:

$$\left.\begin{aligned}\eta &= \lambda(H - \Gamma\cot\beta)\\ \chi &= \lambda X\\ \xi &= \lambda\Gamma\csc\beta\end{aligned}\right\} \quad (14)$$

and the Jacobian of the coordinate transformation is merely $\lambda^3\csc\beta$. Thus, the transformed integral becomes:

$$J_{\text{Bragg}} = \frac{CR^2}{\dot\xi}|f_0|^2 e^{-2M}\lambda^3\csc\beta \times\int_H\int_X\int_\Gamma I_0(\mathbf{S}/\lambda)\,dH\,dX\,d\Gamma \quad (15)$$

and, since it has been assumed that the $\omega$ and/or $\varepsilon$ scan widths will be small, it follows that $\beta$ will be approximately constant. For a pure $\omega$-scan, $\varepsilon = 0$, $\dot\xi$ reduces to $2\,\dot\omega\sin\theta$, and $\beta$ becomes $\frac{\pi}{2} + \theta$, thus equation (15) reduces to the following:

$$J_{\text{Bragg}} = \frac{CR^2}{\dot\omega}|f_0|^2 e^{-2M}\frac{\lambda^3}{\sin(2\theta)} \times\int_H\int_X\int_\Gamma I_0(\mathbf{S}/\lambda)\,dH\,dX\,d\Gamma \quad (16)$$

This is the same expression developed by James (1962; equation 2·36) for an $\omega$ scan. For a standard $\omega/2\theta$ scan, $\varepsilon = \omega$, $\dot\xi$ reduces to $2\dot\epsilon\cos\theta$, and $\beta$ becomes $\theta$; thus the only change necessary in equation (16) is to replace $\dot\omega$ by $\dot\epsilon$.

As noted previously, so long as the region of integration in equation (15) adequately covers the Bragg peak, the result of the integration is independent of the integration limits. This integration is carried out by James (1962) and the results are as follows:

$$J_{\text{Bragg}} = \frac{CR^2}{\dot\xi}|f_0|^2 e^{-2M}\frac{\lambda^3}{\sin\beta}\frac{N}{\tau} \quad (17)$$

where $\tau$ is the volume of a unit-cell in the lattice.

In evaluating the integrated T.D.S. a similar argument is developed and it is only necessary to replace the Laue interference function in equation (15) with $I_{\text{TDS}-1}(\mathbf{S}/\lambda)$, as given in equation (7):

$$J_{\text{TDS}-1} = \frac{CNR^2}{m\dot\xi}|f_0|^2 e^{-2M}\frac{\lambda^3}{\sin\beta}\int_H\int_X\int_\Gamma\sum_{j=1}^{3} \times\left[\left\{\frac{\mathbf{S}}{\lambda}\cdot\hat{\mathbf{e}}\left(\frac{\mathbf{k}}{j}\right)\right\}^2 < E\left(\frac{\mathbf{k}}{j}\right) > \Big/ v\left(\frac{\mathbf{k}}{j}\right)^2\right] dH\,dX\,d\Gamma \quad (18)$$

It will be convenient to work with the ratio of the integrated T.D.S. to the integrated Bragg scattering; using the notation introduced by Nilsson (1957), let this ratio be represented by $\alpha$:

$$\alpha = \frac{J_{\text{TDS}-1}}{J_{\text{Bragg}}} = \frac{1}{\varrho}\int_H\int_X\int_\Gamma\sum_{j=1}^{3} \times\left[\left\{\frac{\mathbf{S}}{\lambda}\cdot\hat{\mathbf{e}}\left(\frac{\mathbf{k}}{j}\right)\right\}^2 < E\left(\frac{\mathbf{k}}{j}\right) > \Big/ v\left(\frac{\mathbf{k}}{j}\right)^2\right] dH\,dX\,d\Gamma \quad (19)$$

where $\frac{m}{\tau}$ has been replaced by the material density, $\varrho$.

Clearly, correction of the measured integrated intensity for T.D.S. is achieved by dividing the measured intensity by the correction factor $(1+\alpha)$.

The vector $\mathbf{g}$ can be described in the previously defined orthogonal coordinate system as follows:

$$\mathbf{g} = H\hat{\mathbf{e}}_H + X\hat{\mathbf{e}}_X + \Gamma\hat{\mathbf{e}}_\Gamma \quad (20)$$

In principle at least, the integral in equation (19) can now be evaluated. For each point within the region of integration (defined by the parameters $H$, $X$, and $\Gamma$), there exists a lattice wave vector; upon evaluation of the three eigenfrequencies and eigenvectors associated with this wave vector, the integrand of equation (19) can be evaluated. Repeating this procedure for a large number of points in the integration region will suffice to evaluate the integral. In practice however, this is not

feasible since specific knowledge of the relation between the wave vectors and their eigenfrequencies and eigenvalues is required. Although this information can be obtained from inelastic neutron scattering data or lattice dynamical force models, it is generally not available.*

The region in reciprocal space, over which the T.D.S. must be evaluated, is centered at a reciprocal lattice point and is small in comparison to the size of the Brillouin zone. Typical integrated intensity measurements considered for a variety of materials involved reciprocal volumes which were less than 1% of the size of the Brillouin zone. Only the long lattice waves (low frequency modes) are considered in the immediate vicinity of a reciprocal lattice point and it is this fact which allows introduction of two approximations: firstly, it is assumed that the continuum approximation can be made, *i.e.* that the lattice wave velocities are independent of frequency. Indeed, in the long wavelength limit, there is no dispersion and this condition is fulfilled exactly. Utilizing this approximation in equation (19) and substituting the average energy expression from equation (4) yields the following equation:

$$\alpha = \frac{h}{2\varrho}\int_H\int_X\int_\Gamma\left[\sum_{j=1}^{3}\left[\left\{\frac{\mathbf{S}}{\lambda}\cdot\hat{\mathbf{e}}\left(\frac{\mathbf{k}}{j}\right)\right\}^2 \times \coth\frac{\left\{hv\left(\frac{\mathbf{g}}{j}\right)|\mathbf{g}|\right\}}{2kT}\Big/\left\{v\left(\frac{\mathbf{g}}{j}\right)|\mathbf{g}|\right\}\right]\mathrm{d}H\mathrm{d}X\mathrm{d}\Gamma\right] \quad (21)$$

where $v\left(\frac{\mathbf{g}}{j}\right)$ is the velocity associated with the normal mode of polarization index $j$ and of wave vector $\mathbf{k}$. The fact that only the low frequency lattice waves are being considered can also be used to justify a second approximation, *viz* that $hv \ll kT$ and hence the average energy of a normal mode involved in this calculation is $kT$. Of course, this condition will be fulfilled for all normal modes in the high temperature region, *i.e.* when the crystal temperature is in excess of its Debye temperature. This approximation allows the expression for $\alpha$ to be written in the following form:

$$\alpha = \frac{kT}{\varrho}\int_H\int_X\int_\Gamma\left[|\mathbf{g}|^{-2}\sum_{j=1}^{3}\left\{\left\{\frac{\mathbf{S}}{\lambda}\cdot\hat{\mathbf{e}}\left(\frac{\mathbf{g}}{j}\right)\right\}^2 v\left(\frac{\mathbf{g}}{j}\right)^{-2}\right\}\mathrm{d}H\mathrm{d}X\mathrm{d}\Gamma\right] \quad (22)$$

Strictly speaking, it is equation (22) which must be evaluated for accurate calculation of the T.D.S. contribution to the measured intensities. However, by making two additional approximations, equation (22) can be reduced to a relatively simple form. The first assumption stems from the fact that, within the continuum approximation, the term in the summation in equation (22) is independent of the magnitude of the wave vector, *i.e.* the wave velocities and their associated polarization vectors will vary only with direction. Therefore, if it is assumed that all directions of propagation are considered with equal probability for each value of $|\mathbf{g}|$, then the summation in equation (22) can be averaged over all directions independently. The weighted mean reciprocal square velocity, $<v^{-2}(\hat{\mathbf{e}}_S)>$, is defined as follows:

$$<v^{-2}(\hat{\mathbf{e}}_S)> = \left[\sum_{j=1}^{3}\left\{\hat{\mathbf{e}}_S\cdot\hat{\mathbf{e}}\left(\frac{\mathbf{g}}{j}\right)\Big/ v\left(\frac{\mathbf{g}}{j}\right)\right\}^2\right]_{\substack{\text{averaged over}\\ \text{all directions}}} \quad (23)$$

where $\hat{\mathbf{e}}_S$ is a unit vector parallel to $\mathbf{S}$. Indeed, it is only when the reciprocal volume, over which the integration is carried out, is spherical in shape that this condition is fulfilled exactly and it is for the larger values of $|\mathbf{g}|$, in the extremes of the integration region, that all propagation directions are not considered. Therefore, the error induced by using $<v^{-2}(\hat{\mathbf{e}}_S)>$ is reduced by the multiplicative factor $|\mathbf{g}|^{-2}$; the size of this error is discussed below.

In the general anisotropic situation, $<v^{-2}(\hat{\mathbf{e}}_S)>$ must be evaluated numerically employing the Christoffel equations. However, if it is further assumed that all values of $\hat{\mathbf{e}}\left(\frac{\mathbf{g}}{j}\right)$ occur with equal probability, as would be the case for the aforementioned spherical volume in a cubic lattice, then the numerator of equation (23) can be averaged separately, yielding a factor of $\frac{1}{3}$. The remaining portion of equation (23), the averages over all directions of the velocity functions, can easily be calculated from elastic constant data. Anderson (1963) has shown that use of an averaging technique, which is a composite of approximations of several authors (Voight, Reuss, Hill and Gilvarry), for the reciprocal cubic averaged velocity leads to results which, for all symmetry classes, are usually accurate to within experimental limits of error in the elastic constant data employed. Extending Anderson's averaging scheme to this situation, an approximate value for the weighted mean reciprocal square velocity can be expressed as follows:

$$<v^{-2}(\hat{\mathbf{e}}_S)> \approx \tfrac{1}{3}\{2<v_t>^{-2} + <v_l>^{-2}\} \quad (24)$$

where $<v_t>$ and $<v_l>$ denote the average transverse and longitudinal velocities respectively. Anderson has related these two average velocities by simple algebraic expressions to the elastic constants for all symmetry classes.* These expressions are as follows:

$$\langle v_t\rangle = \sqrt{G_H/\varrho} \quad \text{and} \quad \langle v_l\rangle = \sqrt{(K_H + 4G_H/3)/\varrho} \quad (25)$$

* Calculations of the T.D.S. are presently underway for zinc, using a modified axially symmetric force model.

* We might point out that there appears to be a misprint in the sign of the $s_{13}$-term for the general expression of the minimum shear modulus by the Reuss approximation in Anderson's paper; we believe the sign should be positive.

where:

$$G_H=\{\tfrac{1}{10}[\tfrac{1}{3}(c_{11}+c_{22}+c_{33})-\tfrac{1}{3}(c_{12}+c_{23}+c_{31})+(c_{44}+c_{55}+c_{66})]+\tfrac{1}{2}\tfrac{5}{7}[4(s_{11}+s_{22}+s_{33})-4(s_{12}+s_{23}+s_{13})+3(s_{44}+s_{55}+s_{66})]^{-1}\} \quad (26)$$

and

$$K_H=\{\tfrac{1}{18}[(c_{11}+c_{22}+c_{33})+2(c_{12}+c_{23}+c_{13})]+\tfrac{1}{2}[(s_{11}+s_{22}+s_{33})+2(s_{12}+s_{23}+s_{13})]^{-1}\} \quad (27)$$

and $c_{ij}$ and $s_{ij}$ are the elastic stiffnesses and compliances, respectively. It is curious to note that the results obtained using equation (24) for a number of cubic materials varied by less than 2% from the results calculated using the average velocity expressions of Zachariasen (1945; equation 4·195) or, equivalently, of Nilsson (1957, p. 250).

The T.D.S./Bragg scattering ratio can now be written in the following form:

$$\alpha_{\text{approx.}}=\frac{4kT}{\varrho}\langle v^{-2}(\hat{\mathbf{e}}_S)\rangle\left(\frac{\sin\theta}{\lambda}\right)^2\times\int_H\int_X\int_\Gamma\left\{\frac{\mathrm{d}H\,\mathrm{d}X\,\mathrm{d}\Gamma}{H^2+X^2+\Gamma^2}\right\} \quad (28)$$

where the fact that $|\mathbf{S}|$ is equivalent to $2\sin\theta$ has been employed.

In order to assay the size of the errors generated by both the high temperature approximation and the introduction of the weighted mean reciprocal square velocity, a typical integrated intensity measurement was considered for the 511 reflection of Cu. At 290 °K the value of $\alpha_{\text{approx.}}$ was calculated from equation (29) and (34), using equations (24) through (27) to evaluate $\langle v^{-2}(\hat{\mathbf{e}}_S)\rangle$; this value for $\alpha_{\text{approx.}}$ was 0·0399. For the same situation, summing over a grid of 68,920 points superimposed over the reciprocal volume, $\alpha$ was computed from equation (21) to be 0·038195 and from equation (22) to be 0·038180. For this particular case then, the high temperature approximation caused an error of less than 0·04% and introduction of the weighted mean reciprocal square velocity expression resulted in an error of less than 5%. Indeed, these errors are quite modest in consideration of the labour saved in using $\alpha_{\text{approx.}}$.

*Evaluation of the integral*

The integrand in equation (28) is symmetric in $\chi$ and therefore only the upper half of the detection window need be integrated over, *i.e.* it is only necessary to consider $0\leq\chi\leq\frac{\Delta\chi}{2}$. Furthermore, recalling that the integration is being split into two parts, namely that corresponding to the region between $W$ and $W''$ and that corresponding to the region between $W$ and $W'$ in Fig. 1, the T.D.S./Bragg scattering ratio can be expressed as follows:

$$\alpha_{\text{approx.}}=\frac{8kT}{\varrho\lambda^3}\langle v^{-2}(\hat{\mathbf{e}}_S)\rangle\sum_{j=1}^{2}\sigma_j \quad (29)$$

$$\sigma_j=\sin^2\theta\int_{\eta'=-\frac{\Delta\eta}{2}+\gamma\cot\beta_j}^{+\frac{\Delta\eta}{2}+\gamma\cot\beta_j}\int_{\chi=0}^{\frac{\Delta\chi}{2}}\int_{\gamma=0}^{\Delta\xi_j\sin\beta_j}[(\eta')^2+\chi^2+\gamma^2]^{-1}\mathrm{d}\eta'\mathrm{d}\chi\mathrm{d}\gamma, \quad (30)$$

where $\sigma_1$ refers to the integration from the peak in one direction and $\sigma_2$ refers to the corresponding integration in the opposite direction; the reciprocal lengths, $H$, $X$, and $\Gamma$, have been replaced by their angular equivalents, $\eta'$, $\chi$, and $\gamma$. From equations (10) and (11) it follows that:

$$\Delta\xi_j=2[\sin^2(\theta+\Delta\varepsilon_j)+\sin^2\theta-2\sin(\theta+\Delta\varepsilon_j)\times\sin\theta\cos(\Delta\omega_j-\Delta\varepsilon_j)]^{1/2} \quad (31)$$

and

$$\beta_j=\frac{\pi}{2}+\theta-\arccos\left\{\frac{4}{\Delta\xi_j}\sin\theta\sin\left(\frac{\Delta\omega_j-\Delta\varepsilon_j}{2}\right)\right\}. \quad (32)$$

$\Delta\varepsilon_1$ and $\Delta\omega_1$ are the total angular displacements as measured from the peak position in one direction and $\Delta\varepsilon_2$ and $\Delta\omega_2$ are the corresponding limits as measured from the peak position in the opposite direction. Clearly, for an angularly symmetric scan, $\Delta\xi_1=\Delta\xi_2$ and $\beta_1=\beta_2$. It is to be noted that $\sigma_j$ is independent of both the diffracting material and the temperature; it depends only on the experimental constants of the intensity measurement, *i.e.* $\sigma_j=\sigma_j(\theta,\Delta\eta,\Delta\chi,\Delta\varepsilon_j,\Delta\omega_j)$.

In general, the integral in equation (30) cannot be completely evaluated analytically. In considering the equivalent situation for simple cubic materials in the case of a pure $\omega$-scan, Nilsson (1957) performed the integration analytically by assuming that the height of the detection window was infinite. More recently, Cooper & Rouse (1968) have reduced the triple integration to a double integral and performed the two final integrations numerically. They have also considered the error involved in approximating to a sphere, the region over which the integration is to be carried out; this approximation also allows analytical evaluation of the T.D.S./Bragg scattering ratio.

In this work, the triple integration indicated in equation (30) will be reduced analytically to a pair of one dimensional integrations which are to be evaluated, for the general case, numerically. In order to reduce the integral, use is made of Gauss's integration theorem, where the argument is taken to be the following:

$$\mathbf{f}=\mathbf{g}/(\mathbf{g}\cdot\mathbf{g})=(\eta'\hat{\mathbf{e}}_H+\chi\hat{\mathbf{e}}_X+\gamma\hat{\mathbf{e}}_\Gamma)/(\eta'^2+\chi^2+\gamma^2). \quad (33)$$

This allows $\sigma_j$ to be written in the following form:

$$\sigma_j=\sin^2\theta\left[\int_{\gamma=0}^{A_j}\{F(D,\gamma\cot\beta_j+C,\gamma)-F(D,\gamma\cot\beta_j-C,\gamma)+G(C,\gamma\cot\beta_j+C,D,\gamma)+G(C,\gamma\cot\beta_j-C,D,\gamma)\}\mathrm{d}\gamma+\int_{\chi=0}^{D}\{F(A_j,B_j+C,\chi)-F(A_j,B_j-C,\chi)\}\mathrm{d}\chi\right] \quad (34)$$

where

$$F(x,y,z)\equiv x/\sqrt{x^2+z^2}\,\tan^{-1}(y/\sqrt{x^2+z^2}) \quad (35)$$

$$G(w,x,y,z)\equiv w/\sqrt{x^2+z^2}\,\tan^{-1}(y/\sqrt{x^2+z^2}) \quad (36)$$

$$\left.\begin{aligned} A_j &= \Delta\xi_j \sin\beta_j \\ B_j &= \Delta\xi_j \cos\beta_j \\ C &= \Delta\eta \\ D &= \Delta\chi \end{aligned}\right\} \quad (37)$$

and, as previously noted, the remaining integration must be performed numerically. Two versions of a computer program to carry out this integration have been run on a C.D.C.–3800 computer; one is written in the Algol-60 language and the other is written in Fortran.

To compensate for background contributions to the measured intensity, the background intensity is often evaluated far from the Bragg peak under investigation and extrapolated under the peak (*cf.* Renninger, 1952; Young, 1961). Similarly to take account of the background in these expressions, the value of $\gamma$ in the denominator of equation (30) is held constant at $\Delta\xi_j \sin\beta_j$ and the integrations over $\eta'$, $\chi$, and $\gamma$ are carried out; this results in the following expression:

$$(\sigma_j)_{\text{bkgnd}} = \sin^2\theta \int_{\chi=0}^{D} \{F(A_j, B_j + C, \chi) - F(A_j, B_j - C, \chi)\}\mathrm{d}\chi \quad (38)$$

Thus, to compensate for a constant background correction to the measured intensity, one need merely delete the last term in equation (34), *i.e.* the integration over $\chi$.

It can be shown that:

$$\int_{x=0}^{\infty} F(a,b,x)\mathrm{d}x = \frac{\pi a}{2}\log\left\{\frac{b}{a}+\sqrt{(b/a)^2+1}\right\}. \quad (39)$$

Therefore, if the height of the detection window is allowed to increase without bound, *i.e.* if $\Delta\chi\to\infty$, then the value of $\sigma_j$, and hence of the T.D.S./Bragg scattering ratio, can be completely determined analytically; the resulting expression is:

$$(\sigma_j)_{\text{inf.}} = \frac{\pi}{2}\sin^2\theta\left[A_j\log\left\{\frac{B_j+C+\sqrt{(B_j+C)^2+A_j^2}}{B_j-C+\sqrt{(B_j-C)^2+A_j^2}}\right\} + C\sin\beta_j\left(\log\left\{\frac{\sqrt{C^2+(2C\cot\beta_j)A_j+A_j^2\csc^2\beta_j}+A_j\csc\beta_j+C\cos\beta_j}{C(1+\cos\beta_j)}\right\} + \log\left\{\frac{\sqrt{C^2-(2C\cot\beta_j)A_j+A_j^2\csc^2\beta_j}+A_j\csc\beta_j-C\cos\beta_j}{C(1-\cos\beta_j)}\right\}\right)\right]. \quad (40)$$

There is one type of integrated intensity measurement for which the T.D.S./Bragg scattering ratio can be completely evaluated analytically without recourse to additional simplifying approximations. Consider an intensity scan for which the wave vector $\left\{\frac{\mathbf{S}'}{\lambda}-\frac{\mathbf{S}}{\lambda}\right\}$ is parallel to $\hat{\mathbf{e}}_\Gamma$; as seen in Fig. 1, this gives rise to a value of $\pi/2$ for $\beta$ and occurs when $\varepsilon$ and $\omega$ fulfill the following relation:

$$\varepsilon^2+(\tan^2\theta-\sin^2\theta)(2\omega\varepsilon-\omega^2)=0\,. \quad (41)$$

In this case, the limits on the integration over $\eta'$ are not variables of the integration. The second condition which must be fulfilled is that the detection window be circular rather than rectangular in shape. Under these conditions, equation (25) takes on the following form:

$$\alpha_{\text{approx.}} = \frac{4kT}{\varrho\lambda^3}\langle v^{-2}(\hat{\mathbf{e}}_S)\rangle \sin^2\theta \times \sum_{j=1}^{2}\left\{\int_{\varphi=0}^{2\pi}\int_{\psi=0}^{\Delta\psi}\int_{\gamma=0}^{\Delta\xi_j}\frac{\psi\,d\psi\,d\varphi\,d\gamma}{\psi^2+\gamma^2}\right\}, \quad (42)$$

where $\Delta\psi$ is the angular radius of the detection window; integration of equation (42) yields the following expression:

$$\alpha_{\text{approx.}} = \frac{8\pi kT}{\varrho\lambda^3}\langle \mathbf{v}^{-2}(\hat{\mathbf{e}}_S)\rangle \sin^2\theta \times \sum_{j=1}^{2}\left[\Delta\psi \arctan\left(\frac{\Delta\xi_j}{\Delta\psi}\right) + \Delta\xi_j \log\left\{\frac{\sqrt{(\Delta\psi)^2+(\Delta\xi_j)^2}}{\Delta\xi_j}\right\}\right]. \quad (43)$$

It will be shown in the following section that, for low order reflections ($\theta \lesssim 40°$), the T.D.S. contribution to the measured intensity does not vary significantly with the type of intensity scan. Thus, for such cases, equation (43) can provide a relatively quick estimate of the size of the T.D.S. contribution involved.

## Discussion

*Comparison with other calculations and experimental results.*

The results of the calculations in this work are compared with the calculations of Nilsson (1957) and the measurements of Renninger (1966) for NaCl in Table 1; in all cases, the background correction has been applied.

When the infinite slit height approximation is made [equation (40)], the results of this work are in excellent agreement with Nilsson's calculations for both NaCl and KCl. As this agreement implies, the evaluation of the mean reciprocal square velocity, $\langle v^{-2}(\hat{\mathbf{e}}_S)\rangle$, as determined in this work, is essentially equivalent to the technique employed by Nilsson for NaCl and KCl.

It is to be noted that equation (24) is generally applicable under the aforementioned approximations. However, as Schwartz (1964) has pointed out, the approximate formula given by Nilsson cannot be applied for many materials. More specifically, when:

$$-(c_{11}-c_{12}-2c_{44})\,(c_{11}+c_{12})c_{44}>0$$

and

$$-(c_{11}+c_{12})c_{44}<(c_{11}-c_{12}-2c_{44})\,(c_{11}+2c_{12}-c_{44})$$

there is a singularity in the expression for the mean velocity which must properly be accounted for in subsequent integrations; for such cases, an integration technique such as that proposed by Schwartz must be used.*

Table 1. *Comparison of calculated values of* $\alpha$ *with Nilsson's* (1957) *calculations and Renninger's* (1966) *measurements for* NaCl

| $h$ | $k$ | $l$ | Nilsson | This work $\Delta\chi=\infty$ | This work $\Delta\chi=5°$ | Experiment |
|---|---|---|---|---|---|---|
| 2 | 2 | 2 | 0·015 | 0·0157 | 0·0156 | |
| 4 | 0 | 0 | 0·024 | 0·0239 | 0·0237 | |
| 6 | 0 | 0 | 0·077 | 0·0766 | 0·0751 | |
| 6 | 2 | 2 | 0·103 | 0·1014 | 0·0991 | |
| 4 | 4 | 4 | 0·117 | 0·1144 | 0·1106 | |
| 8 | 0 | 0 | 0·171 | 0·1692 | 0·1641 | |
| 6 | 4 | 4 | 0·183 | 0·1835 | 0·1777 | |
| 8 | 2 | 0 | 0·183* | 0·1835 | 0·1777 | 0·20 ± 10% |
| 8 | 2 | 2 | 0·197 | 0·1980 | 0·1915 | |
| 10 | 0 | 0 | 0·302 | 0·3019 | 0·2895 | |
| 10 | 2 | 0 | 0·320* | 0·3169 | 0·3036 | 0·31 ± 20% |
| 6 | 6 | 6 | 0·337 | 0·3318 | 0·3176 | |

Experimental conditions: $\Delta\eta=5°$; $\Delta\omega_1=\Delta\omega_2=1·5°$; $\Delta\varepsilon_1=\Delta\varepsilon_2=0°$; $\lambda=0·71$ Å; $T=290°$K

* Value reported by Renninger (1966).

The values given in column 3 of Table 1 represent the T.D.S./Bragg scattering ratio presuming that the detection window is square, *i.e.* the true height of the X-ray detection window was given neither by Nilsson (1957) nor Renninger (1952, 1966). Thus the difference between columns 2 and 3 in Table 1 would represent the error involved in making the infinite window height approximation, if the detection window had had an angular height of 5°.

The recent experimental results of Renninger (1966) for NaCl are given in column 4 of Table 1; Renninger's data for the 822 reflection of Si give a value of 0·056 ± 20% for $\alpha$. This result for Si is to be compared with 0·0473 as calculated from equations (29) and (34). Although the data are limited, they do appear to confirm the theory. It should be noted however, that application of either Nilsson's formulae or the expressions of this work to either NaCl or Si is an approximation, *i.e.* strictly speaking, both calculations were

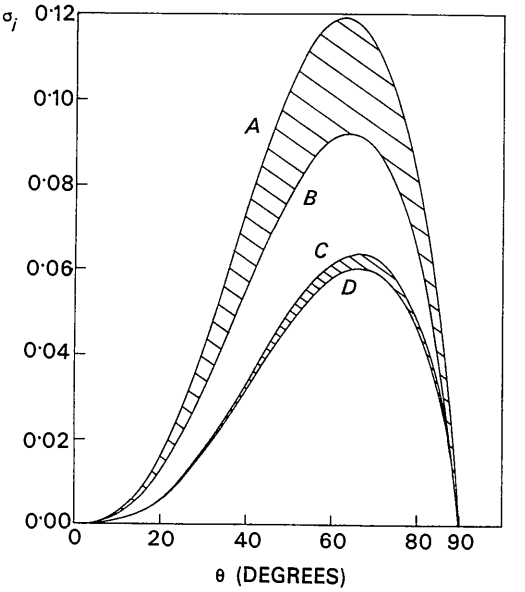


Fig. 2. Plot of $\sigma_j$ versus diffraction angle, $\theta$, for four different experimental situations. [$\Delta\eta=\Delta\chi=5·0°$; $\Delta\varepsilon_j=0·0°$; $\Delta\omega_j=1·5°$]. Curve *A*: Total intensity measurement; infinite slit height. Curve *B*: Total intensity measurement; square detection window. Curve *C*: Constant background correction; infinite slit height. Curve *D*: Constant background correction; square detection window.

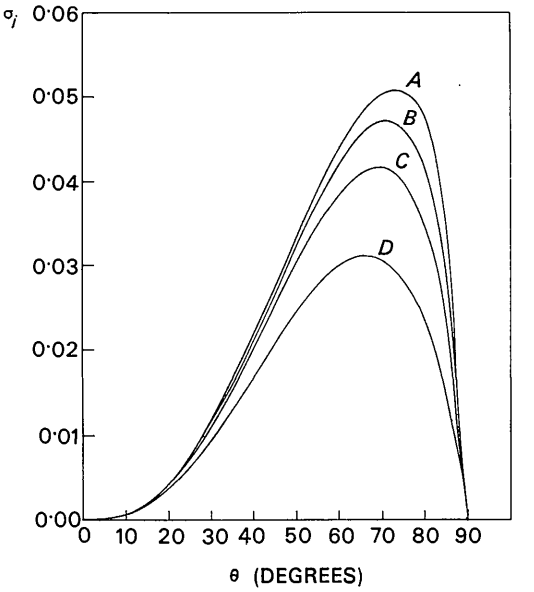


Fig. 3. Plot of $\sigma_j$ *versus* diffraction angle, $\theta$, for increasing $\omega/2\theta$-scan widths. [$\Delta\eta=\Delta\chi=1·5°$]. Curve *A*: $\Delta\varepsilon_j=\Delta\omega_j=2·0°$. Curve *B*: $\Delta\varepsilon_j=\Delta\omega_j=1·5°$. Curve *C*: $\Delta\varepsilon_j=\Delta\omega_j=1·0°$. Curve *D*: $\Delta\varepsilon_j=\Delta\omega_j=0·5°$.

* *Note added in proof*: – Walker & Chipman (1969) have very recently examined the general applicability of Nilsson's expression for the mean reciprocal square velocity and have discussed an error which was apparently made in Schwartz's calculations.

developed for monatomic lattices. It is also possible that the slight discrepancy seen for the 820 reflection of NaCl might be due to higher order T.D.S. effects which are not considered in either this calculation or Nilsson's.

Annaka (1962) has also derived an expression to evaluate the T.D.S./Bragg scattering ratio for an $\omega$ scan. In essence, he has made some approximations concerning the region in reciprocal space over which the integration indicated in equation (28) is to be carried out and, in so doing, he has reduced the basic expressions for the T.D.S./Bragg scattering ratio to a tenable form. Annaka has reported values for the T.D.S./Bragg scattering ratio for NaCl, $\alpha$-Fe, and anthracene. An evaluation of what we believe to be the same situation for NaCl and $\alpha$-Fe, using the expressions of this work [equations (29) and (34)], yielded results which were about 50% lower than those reported by Annaka (1962). However, Annaka (1968) has recently recomputed the T.D.S./Bragg scattering ratio for NaCl and $\alpha$-Fe; our agreement with these calculations is quite good. The differences between Annaka's (1968) results and the results of this work are of the order of a few per cent and are probably due to the different methods of evaluating the integral over the reciprocal volume 'seen' during the intensity scan.

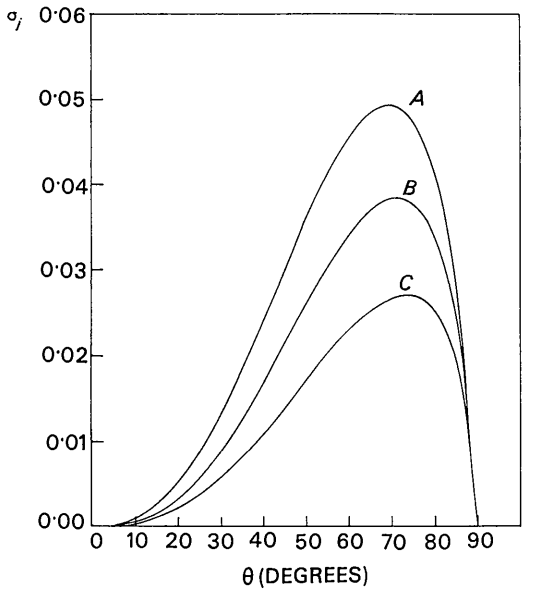


Fig. 4. Plot of $\sigma_j$ *versus* diffraction angle, $\theta$, for increasing detection window widths. [$\Delta\chi = 1{\cdot}5°$; $\Delta\varepsilon_j = \Delta\omega_j = 1{\cdot}25°$]. Curve $A$: $\Delta\eta = 2{\cdot}0°$. Curve $B$: $\Delta\eta = 1{\cdot}0°$. Curve $C$: $\Delta\eta = 0{\cdot}5°$.

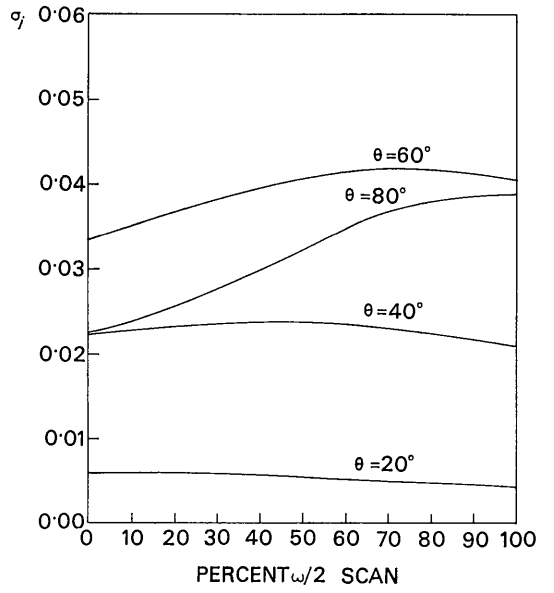


Fig. 5. Plot of $\sigma_j$ *versus* type of intensity scan for four diffraction angles. [$\Delta\eta = \Delta\chi = 1{\cdot}5°$].

*Examination of the variation of the T.D.S./Bragg scattering ratio.*

As previously noted, the T.D.S./Bragg scattering ratio can be described through the dimensionless quantity $\sigma_j$. In Fig. 2 the variation of $\sigma_j$ with diffraction angle, $\theta$, has been plotted for four different situations. The two upper curves represent the total measured T.D.S./Bragg scattering ratio for an infinitely high detector window (curve $A$) and for a square detection window (curve $B$). The cross-hatched region between curves $A$ and $B$ represents the error introduced in making the infinite slit height approximation for this particular situation; this amounts to a 30% error at the maximum. In curves $C$ and $D$ of Fig. 2, similar plots are shown, however these results have been corrected for a constant background contribution. Again, the cross-hatched region represents the error involved in making the infinite window height approximation for this situation. At the peak, this corresponds to an error which is less than 6%. Indeed, as stated by Nilsson (1957, p. 255), the inclusion of the background correction serves to reduce significantly the error involved in assuming the X-ray detection window to be infinitely high.

It is quite obvious from these curves that the effect of the T.D.S. on the measured intensity increases to a rather pronounced maximum in the intermediate-high angle region and drops rapidly to zero as $\theta$ approaches 0° and 90°. The reason why the T.D.S. contribution vanishes at these two extremes is linked to the fact that the reciprocal volume 'seen' during the intensity measurement tends to vanish in these regions.

In Fig. 3 the variation of $\sigma_j$ with diffraction angle has been plotted for four different $\omega/2\theta$ scan widths. As expected, the increase in $\sigma_j$ realized, as the size of the intensity scan is increased, tends to become less and less. This is of course due to the fact that the T.D.S. is also peaked at the Bragg peak position, thus an increased scan width serves to include more and more of a decreasing tail. It is curious to note however,

that the peak value of $\sigma_j$ does tend to shift slightly to a higher $\theta$ value as the scan size is increased.

The variation of $\sigma_j$ with diffraction angle has been plotted for three different X-ray detection window widths in Fig. 4. As in the previous case, the net increase in $\sigma_j$ appears to diminish as the window width is increased. This too is due to the fact that the T.D.S. itself is peaked at the Bragg diffraction peak and again, one is merely 'seeing' more and more of a diminishing tail.

Recognizing that the T.D.S./Bragg scattering ratio tends to show a pronounced maximum (at least for the situations considered in this work) in the high angle region, ($60° \lesssim \theta \lesssim 80°$) attempts to measure the T.D.S. contribution experimentally would perhaps be most fruitful if performed on Bragg reflections lying in this region.

Finally, in Fig. 5, the variation of $\sigma_j$ is examined as the type of intensity scan is changed from a pure $\omega$ scan (crystal only rotating) to a pure $\omega/2\theta$ scan (crystal and counter simultaneously rotating in a 1:2 ratio) for four different diffraction angles. As evidenced by the curves in Fig. 5, for low order reflections ($40° \lesssim \theta$), the T.D.S./Bragg scattering ratio does not vary significantly as the type of intensity scan is changed from a pure $\omega$ scan ($\beta = \pi/2 + \theta$) to a pure $\omega/2\theta$ scan ($\beta = \theta$). For higher order reflections however ($\theta \gtrsim 60°$), the effect of changing the type of intensity scan is quite pronounced: for $\theta = 80°$, a 73% increase in the value of $\sigma_j$ is realized as $\beta$ decreases from $\pi/2 + \theta$ to $\theta$. It should be noted, though, that if equation (24) had not been used to evaluate $\langle v^{-2}(\hat{\mathbf{e}}_S)\rangle$, this variation of the T.D.S./Bragg scattering ratio with the type of scan could be somewhat more pronounced due to possible anisotropic effects.

The curves shown in Fig. 5 tend to suggest that experiments designed to measure the effect of T.D.S. should be performed using an intensity scan which represents an admixture of the $\omega$ scan and the $\omega/2\theta$ scan, *i.e.* the crystal and detector should be simultaneously rotated in a ratio which tends to maximize $\sigma_j$.

## Conclusions

A technique for evaluating the first order T.D.S. contribution to integrated X-ray intensity measurements of Bragg reflections for monatomic crystalline lattices has been developed. The calculation has been carried out for a general type of diffractometer integrated intensity measurement; the special cases where only the crystal is rotating ($\omega$ scan), and where the crystal and detector are simultaneously rotating in a 1:2 ratio ($\omega/2\theta$ scan) are considered. The equations appropriate to a constant background correction are given and simplified expressions are presented for the special case of an infinitely high detection window and for a circular detection window moving in reciprocal space in a direction perpendicular to the Ewald sphere of reflection. It was found, for the typical situations considered, that when the infinite slit approximation is applied, the error involved can be significantly reduced (from as much as 30% to less then 6%) by applying a constant background correction; this is in agreement with Nilsson's (1957) prediction.

The calculated results for the T.D.S./Bragg scattering ratio for a typical situation using the final expressions of this work, equations (29) and (34), were compared with the answers obtained *via* a rigorous numerical integration of the basic expressions. This comparison showed that, for the situation considered, the errors introduced by the high temperature approximation and the averaging expression for $\langle v^{-2}(\hat{\mathbf{e}}_S)\rangle$ were less than 5%. Furthermore, the results of this calculation are in excellent agreement with Nilsson's (1957) results for both NaCl and KCl and in good agreement with Annaka's (1968) calculations for NaCl and α-Fe. These facts represent a partial check on the more general expressions used in this work.

Limited experimental confirmation of the results of this calculation has been obtained by comparison with the measurements of Renninger (1966) on NaCl and Si.

Finally, the effect of the T.D.S. contribution to the measured intensity was investigated through a dimensionless parameter, $\sigma_j$, which depends only on the experimental constants relating to the intensity measurements. It was found that $\sigma_j$ vanishes as the diffraction angle approaches 0° and 90°; in an intermediate-high angle region ($60° \lesssim \theta \lesssim 80°$), $\sigma_j$ tends to show a very pronounced maximum. Increasing the size of either the X-ray detection window or the width of the intensity scan, both serve to increase $\sigma_j$, but in increasingly smaller amounts. For low order reflections ($\theta \lesssim 40°$), the T.D.S. contribution to the measured intensity is relatively insensitive to the type of intensity scan, but for higher order reflections ($\theta \gtrsim 60°$), this contribution shows an increasing variation as the intensity scan is changed from a pure $\omega$ scan to a pure $\omega/2\theta$ scan.

The authors would like to express their thanks to Dr Joseph L. Feldman, Dr B. T. M. Willis, and Dr Forrest L. Carter for their interest in this work. We are also grateful to Professor M. Renninger for his assistance in the evaluation of α for Si and to Dr M.J. Cooper and Mr K. D. Rouse for providing a preprint of their paper on T.D.S.

## References

ANDERSON, O. L. (1963). *J. Phys. Chem. Solids*, **24**, 909.
ANNAKA, S. (1962). *J. Phys. Soc. Japan*, **17**, 846; (1968) Private communication.
BORN, M. (1943). *Rep. Prog. Phys.* **9**, 294.
CHIPMAN & PASKIN. (1959). *J. Appl. Phys.* **30**, 1992.
COOPER, D. M. & ROUSE, K. D. (1968). *Acta Cryst.* A **24**, 405.
JAMES, R. W. (1962). *The Optical Principles of the Diffraction of X-Rays*. London: Bell.

MARADUDIN, A. A., MONTROLL, E. W. & WEISS, G. H. (1963). *Solid State Physics*, Suppl. 3, edited by SEITZ and TURNBULL, p. 231. New York: Academic Press.
NICKLOW, R. M. & YOUNG, R. A. (1964). Tech. Rept. No. 3, ONR Contract No. NOnr 991(00) and 991(06); NR-017-623, with Georgia Institute of Technology.
NILSSON, N. (1957). *Ark. Fys.* **12**, 247.
RENNINGER, M. (1952). *Acta Cryst.* **5**, 711.
RENNINGER, M. (1966). *Advanc. X-Ray Anal.* **10**, 42.
SCHWARTZ, L. H. (1964). *Acta Cryst.* **17**, 1614.
WALKER, C. B. & CHIPMAN, D. R. (1969). *Acta Cryst.* A**25**, in the press.
WALLER, I. (1925). Uppsala Dissertation, pp. 1–58.
WALLER, I. (1928). *Z. Phys.* **51**, 213.
WARREN, B. E. (1953). *Acta Cryst.* **6**, 803.
YOUNG, R. A. (1961). Tech. Rept. No. 2, ONR Contract No. NOnr 991(00) and 991(06); NR-017-623, with Georgia Institute of Technology.
ZACHARIASEN, W. H. (1945). *Theory of X-Ray Diffraction in Crystals*. New York: John Wiley.

*Acta Cryst.* (1969). A**25**, 329

# Magnetic Symmetry Groups

BY T. S. G. KRISHNAMURTY AND P. GOPALAKRISHNAMURTY
*Andhra University, Waltair, S. India*

(*Received* 20 *April* 1968 *and in revised form* 17 *September* 1968)

It is shown that the real one-dimensional irreducible representations of a crystallographic point group induce the magnetic symmetry groups associated with the point group and also give the number of independent non-vanishing constants required to describe any magnetic property for the induced magnetic symmetry groups.

## 1. Introduction

The crystallographic point groups describe the spatial symmetry operations like rotations and rotation-reflexions by which a crystal is brought into coincidence with itself. By the application of an ordinary symmetry operation on an arrangement of atoms in a point group, although the geometrical structure may be brought into coincidence with itself, it may be that the orientations of some or all of the atomic magnetic moments (spins) are reversed. In such a case a further reversal of the affected spins must follow the usual symmetry operation in order to bring the geometrical structure, together with the spins, into complete coincidence with itself. The time reversal operation, $\mathscr{R}$, has been introduced in this context to account for the reversal of the spins. The need for generalization of the concept of symmetry operations was realized long ago by Shubnikov (1951), Landau & Lifshitz (1960) and several others to explain the magnetic properties of crystals. The introduction of the new symmetry operation $\mathscr{R}$ increases the number of the point groups from 32 to 122. These 122 point groups can be classified broadly into two categories. They are (i) the 32 grey groups containing $\mathscr{R}$ explicitly and (ii) the 90 magnetic symmetry groups. The 32 conventional crystallographic point groups together with the 58 bicoloured magnetic point groups constitute the 90 magnetic symmetry groups. The magnetic symmetry groups have been derived in a variety of ways by Shubnikov (1951), Tavger & Zaitsev (1956), Hamermesh (1962), Tinkham (1964) and Bhagavantam & Pantulu (1964). Recently Koptsik (1966) also discussed the magnetic symmetry groups in connexion with the description of magnetic structures of crystals on the basis of Landau's theory of the second order phase transitions. In this paper it is proposed to derive the magnetic symmetry groups by a more elegant method, based on the representation theory of groups. The method presented here emphasizes the significance of the physical constants occurring in the alternating representations of the conventional point groups, and this is explained in § 4.

## 2. Description of the method

The magnetic symmetry groups have been constructed (Hamermesh, 1962) by selecting possible subgroups of index 2 from the 32 point groups. A subgroup $H$ of index 2 of a group $G$ is necessarily a self-conjugate subgroup of $G$. Then $G$ can be written as $G=H+A_iH$, where $A_i$ is any element that belongs to $G-H$. The co-sets $H$ and $A_iH$ form the factor group $G/H$. Constructing the set $M_{(G)H}$ of elements associated with the group $G$ defined by the relation $M_{(G)H}=H+\mathscr{R}A_iH$, it can be seen that $M_{(G)H}$ forms a group, which is called the magnetic group of $G$ with respect to $H$. Thus in the construction of the magnetic groups of $G$, one has $A_i^2H=H$ so that the characters of $A_iH$ in the factor group $G/H$ are $\pm 1$. Hence the representations of $A_iH$ in the factor group are real and one-dimensional. Given a subgroup $H$ of index 2 of $G$, there corresponds uniquely to it a real one-dimensional